Prediction of thermodynamic properties of krypton by Monte Carlo simulation using *ab initio* interaction potentials

Afshin Eskandari Nasrabad and Ulrich K. Deiters[a)]
Institute of Physical Chemistry, University of Cologne, Luxemburger Str. 116, D-50939 Köln, Germany

The vapor–liquid equilibria of pure krypton were calculated by Gibbs ensemble Monte Carlo simulation using two different *ab initio* pair potentials. One pair potential was obtained from coupled-cluster calculations, using the CCSD(T) level of theory and two successive correlation consistent basis sets, aug-cc-pVTZ and -pVQZ. The resulting pair potentials were extrapolated to obtain the basis set limit of the interaction energies. The second *ab initio* potential was taken from literature. It is shown that the coupled-cluster potential leads to a quantitative prediction of second virial coefficients, vapor pressures, and orthobaric densities, if Axilrod–Teller triple-dipole potentials are included in the simulations. © *2003 American Institute of Physics.*
[DOI: 10.1063/1.1579671]

I. INTRODUCTION

Knowledge of phase equilibria and related properties of fluids is important in many fields of science and industry. While the calculation of such properties has been almost entirely the domain of equations of state during the previous decades, the rapid increase of computational resources has made molecular simulations an attractive alternative for such calculations, especially because computer simulations do not need to make as many simplifying assumptions about the molecular interaction potentials as equations of state and because they are not only able to provide thermodynamic equilibrium data, but also nonequilibrium data.[1]

However, computer simulations require intermolecular interaction potentials as input. Until now, the potentials used have almost exclusively been empirical or semiempirical functions. While such potentials have proven very useful in the past, some limitations are evident:

(1) The potential parameters are valid only for the ranges of state variables (temperature, density, ...) of the experimental data to which they had been fitted.
(2) In the case of mixtures combining rules must be applied which may not be accurate.
(3) ''United atom'' pair potentials may not properly the reflect the anisotropy of the molecular interaction potentials.

In contrast to these empirical approaches, intermolecular potentials based on *ab initio* quantum mechanical methods have no such limitations, and with the recently available computational resources it should be possible to calculate the interaction energies for small and medium-sized molecules with sufficiently high accuracy.

It is objective of this work to combine *ab initio* pair potentials for krypton with computer simulations in order to generate thermodynamic data without a prior knowledge of experimental data. For such an approach the term *global simulation* has been coined.[2–4] It involves the following steps:

(1) the calculation of interaction energies between two krypton atoms for a sufficient number of distances by standard quantum mechanical methods;
(2) the representation of these energies by an appropriate analytical interpolation function;
(3) and finally Monte Carlo computer simulations to obtain the vapor–liquid equilibria and other thermodynamic properties of krypton.

While nowadays the application of quantum mechanical methods to systems undergoing hydrogen bonding or complex is already well established, the calculation of dispersion forces is much more difficult, because these depend on electron correlation effects. The calculation of such effects cannot be accomplished with Hartree–Fock-type methods; instead, it is necessary to use post-SCF methods like Møller–Plesset perturbation theory, configuration interaction (CI) methods, or coupled-cluster methods. The calculation of the pair potential of krypton, where only dispersion forces are present, is a special computational challenge.

It is known, of course, that the intermolecular interactions between krypton atoms cannot be completely represented by pair potentials. In this work the effect of three-body effects is also studied.

II. INTERACTION POTENTIALS

An accurate calculation of the interaction potential of the krypton dimer is rather difficult because of the existence of the fully occupied *d*-shell in the krypton atoms. As a result, publications of high-level *ab initio* calculations for the krypton interaction potential are scarce, and to our knowledge the only one reported so far is by Tao.[5] In that report, quantum mechanical perturbation theory (frozen-core MP4) and various basis sets including bond functions were used. The best

a)Author to whom correspondence should be addressed. Electronic mail: deiters@xenon.pc.uni-koeln.de

TABLE I. Results of the quantum mechanical calculations for the pair potential of the krypton dimer.

	$\phi(R)/\mu E_h$				
$R/\text{Å}$	CCSD(T) aug-cc-pVTZ	CCSD(T) aug-cc-pVQZ	CCSD(T) aug-cc-pV∞Z	MP4[a] $4d2\,f$-$\{2d1f\}$	MP4[a] $4d3f$-$\{2d1f\}$
3.0	12463.2	11316.8	10480.2	11092.4	10905.2
3.2	5578.2	4783.0	4202.7	4607.2	
3.4	2172.5	1632.0	1237.6	1491.3	1433.9
3.6	567.7	211.2	−47.2	96.0	
3.8	−129.4	−357.1	−523.3	−452.5	−468.5
4.0	−384.9	−527.2	−631.0	−604.6	−612.8
4.2	−437.6	−525.7	−590.0	−585.8	−590.0
4.4	−405.9	−461.0	−501.2	−505.3	
4.6	−346.1	−381.5	−407.3	−412.7	−414.2
4.8	−283.5	−307.0	−324.2	−328.0	
5.0	−227.5	−243.7	−255.5	−257.4	−258.2
6.0	−74.7	−77.5	−79.5	−77.0	−77.8
8.0	−12.2	−12.3	−12.4	−11.0	−11.0
10.0	−3.1	−3.1	−3.1	−2.7	−2.7

[a]Reference 5.

results were obtained with the $4d3f$-$\{2d1f\}$ basis set (denoting a $[9s7p4d3f]$-$\{3s3p2d1f\}$ basis set; abbreviations are according to Ref. 5). The predicted well depth of the intermolecular potential is 617 μE_h (Hartree units).

We have now developed a new *ab initio* potential for the krypton dimer, using the coupled-cluster method [CCSD(T) level of theory] and two successive correlation-consistent basis sets, aug-cc-pVTZ and aug-cc-pVQZ. The calculations were carried out at 14 different interatomic distances ranging from 3.0 to 10.0 Å. The basis set superposition error was corrected with the counterpoise method of Boys and Bernardi.[6] The $1/X^3$ extrapolation method[7] was then used to calculate the basis set limit (aug-cc-pV∞Z) of the interaction energies. The resulting values of the pair potential as well as two of the results of Tao[5] (frozen-core MP4 perturbation

theory and $4d2\,f$-$\{2d1f\}$ and $4d3f$-$\{2d1f\}$ basis sets) are shown in Table I. Figure 1 displays these potentials and compares them with the empirical potential of Aziz and Slaman.[8]

Both MP4 potentials are more repulsive at the atomic core than the empirical potential, and more attractive beyond the potential well minimum. The newly developed aug-cc-pV∞Z pair potential shows a better overall agreement with the empirical potential; it is better than both MP4 potentials at the atomic core as well as at larger distances.

The depths and positions of the minima of the pair potentials discussed here are shown in Table II. The minimum of the aug-cc-pV∞Z potential is located at a distance only about 0.22% larger than that of the empirical potential, and the well depth is too small by only 0.88%. These figures confirm that the aug-cc-pV∞Z potential is indeed of high quality, and that the $1/X^3$ extrapolation method is a reliable way to estimate the basis set limit. In contrast to the new pair potential the two MP4 potentials have larger deviations of the well depths and well positions.

In order to obtain an analytical representation of the pair potential, we fitted the tabulated potential energies to a mathematical form proposed by Korona *et al.*,[9] which includes a repulsive exponential term and an attractive damped dispersion component of the form,

$$\phi(R) = Ae^{-\alpha R + \beta R^2} + \sum_{n=3}^{5} f_{2n}(R,b) \frac{C_{2n}}{R^{2n}}, \tag{1}$$
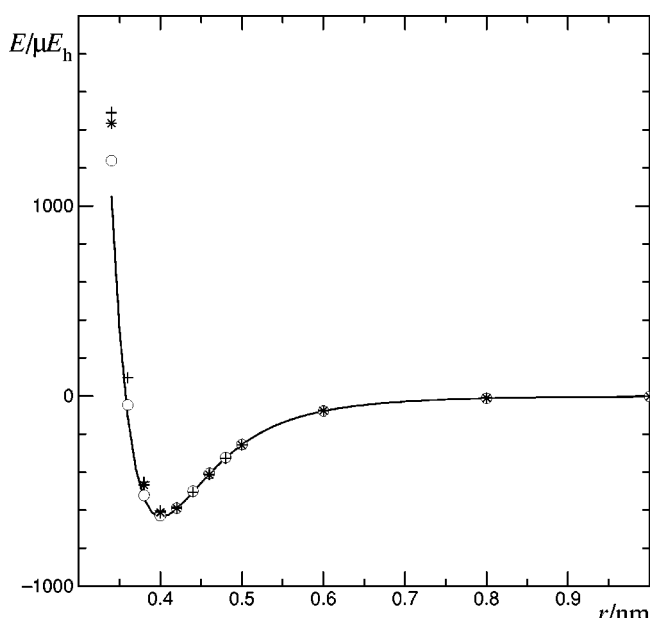
FIG. 1. Potential energy function of the krypton dimer. $\bigcirc$, aug-cc-pV∞Z potential (this work); $+$, $4d2\,f$-$\{2d1f\}$ potential (Ref. 5); $*$, $4d3f$-$\{2d1f\}$ potential (Ref. 5); —, empirical potential (Ref. 8).

TABLE II. Location of the minimum of the krypton pair potential.

Potential	$R_e/\text{Å}$	$\epsilon/\mu E_h$	Ref.
CCSD(T), aug-cc-pV∞Z	4.017	631.55	This work
MP4, $4d2\,f$-$\{2d1f\}$	4.078	609.80	Tao[a]
MP4, $4d3f$-$\{2d1f\}$	4.058	617.00	Tao[a]
Experiment	4.008	637.17	Aziz and Slaman[b]

[a]Reference 5.
[b]Reference 8.

TABLE III. Parameters of the krypton pair potentials [Eq. (1)]. The Hartree energy unit, $E_h = m_c e^4/(4h^2\epsilon_0^2)$, and the Bohr radius, $a_0 = h^2\epsilon_0/(\pi m_c e^2)$, have been used to render the parameters dimensionless.

Parameter	aug-cc-pV∞Z	$4d2\,f$-$\{2d1f\}$
A/E_h	109.66	106.83
αa_0	1.32512	1.36966
βa_0^2	−0.0404	−0.0280
$b a_0$	1.40	1.45
$C_6 a_0^6/E_h$	120.14	90.95
C_8^8/E_h	3565.02	5776.58
C_{10}^{10}/E_h	364467.0	487994.8

where A, α, β, and b denote adjustable parameters, the C_{2n} dispersion coefficients, and f_{2n} the damping functions of Tang and Toennies,[10]

$$f_{2n}(R,b) = 1 - e^{-bR}\sum_{k=0}^{2n}\frac{(bR)^k}{k!}. \qquad (2)$$

The fitting parameters are listed in Table III.

As a first test of quality, the aug-cc-pV∞Z potential was used to calculate second virial coefficients of krypton in the temperature range 100–1050 K from the following equation:

$$B_2(T) = -2\pi N_A \int_0^\infty \left[\exp\left(-\frac{\phi(R)}{k_B T}\right) R^2\right] dR, \qquad (3)$$

where k_B denotes Boltzmann's constant, T is the temperature, N_A is Avogadro's constant, and $\phi(R)$ is the pair potential. The resulting second virial coefficients are compared with experimental data[11] in Fig. 2. The agreement of the calculated and experimental virial coefficients is very good over the whole temperature range.

According to the analysis of Bukowski and Szalewicz,[12] which is confirmed by our experience,[3,4] three-body forces can be accounted for by the Axilrod–Teller (AT) triple-dipole potential,[13]
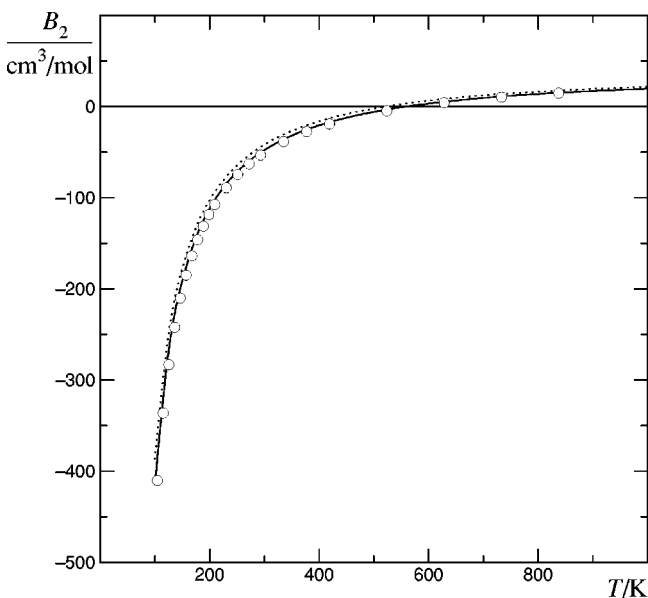

FIG. 2. Second virial coefficients of krypton —, calculated *ab initio* from the aug-cc-pV∞Z potential (this work); ····, $4d2\,f$-$\{2d1f\}$ potential (Ref. 5); ○, experimental data (Ref. 11).

$$E_{AT} = \nu\,\frac{1 + 3\cos\alpha\cos\beta\cos\gamma}{R_{12}^3 R_{23}^3 R_{31}^3}, \qquad (4)$$

where ν is the nonadditivity coefficient which can be calculated from the properties of the monomers ($\nu \approx \frac{9}{16}Va^3$, where V and a are the atomic ionization potential and polarizability, respectively); R_{12}, R_{23}, and R_{31} are the lengths of the sides, and α, β, and γ the angles of the triangle formed by the molecules. In this work the three-body nonadditivity coefficient of krypton was set to 2.20×10^{-17} J Å^9.[14]

III. SIMULATION DETAILS

Constant NVT Gibbs ensemble Monte Carlo simulations[15] were performed with 500 krypton atoms in two cubic

TABLE IV. Vapor–liquid equilibria of krypton. Simulation results obtained with the aug-cc-pV∞Z pair potential without three-body corrections: densities, molar internal energies, vapor pressure, chemical potential, and molar enthalpies of the coexisting phases.

T/K	$\rho/\text{mol dm}^{-3}$	$U_m/\text{kJ mol}^{-1}$	p/MPa	$\mu/\text{kJ mol}^{-1}$	$H_m/\text{kJ mol}^{-1}$
140(g)	0.19(1)	−0.087(8)	0.22(2)	−16.984(75)	1.032(7)
140(l)	28.59(24)	−8.265(86)	−0.23(96)	−16.529(576)	−8.276(70)
150(g)	0.48(6)	−0.210(25)	0.54(6)	−17.343(128)	0.926(37)
150(l)	27.82(37)	−7.972(131)	−0.70(66)	−16.892(457)	−7.977(124)
160(g)	0.66(11)	−0.270(42)	0.77(11)	−18.280(162)	0.919(69)
160(l)	26.81(21)	−7.632(66)	0.37(89)	−18.279(242)	−7.621(60)
170(g)	1.12(10)	−0.448(33)	1.30(10)	−18.943(81)	0.730(51)
170(l)	25.73(8)	−7.244(29)	1.00(50)	−18.864(97)	−7.209(43)
180(g)	1.49(19)	−0.574(83)	1.80(20)	−19.861(118)	0.626(122)
180(l)	24.49(30)	−6.836(92)	1.70(40)	−19.849(79)	−6.771(96)
190(g)	2.26(29)	−0.841(116)	2.60(20)	−20.660(101)	0.320(171)
190(l)	23.16(43)	−6.425(114)	2.50(50)	−20.685(118)	−6.320(116)
200(g)	3.75(23)	−1.358(93)	3.80(10)	−21.433(32)	−0.346(129)
200(l)	21.80(21)	−5.994(65)	3.60(80)	−21.501(90)	−5.834(87)
210(g)	5.30(18)	−1.782(71)	5.00(10)	−22.347(13)	−0.837(110)
210(l)	19.58(45)	−5.368(129)	4.60(70)	−22.433(93)	−5.140(11)

TABLE V. Vapor–liquid equilibria of krypton. Simulation results obtained with the aug-cc-pV∞Z pair potential with three-body corrections: densities, molar internal energies, vapor pressure, chemical potential, and molar enthalpies of the coexisting phases.

T/K	ρ/mol dm^{-3}	U_m/kJ mol^{-1}	p/MPa	μ/kJ mol^{-1}	H_m/kJ mol^{-1}
140(g)	0.37(4)	−0.174(17)	0.40(3)	−16.324(86)	0.898(25)
140(l)	26.78(11)	−7.369(33)	−0.02(17)	−16.215(87)	−7.371(35)
150(g)	0.61(5)	−0.268(22)	0.67(5)	−17.099(76)	0.837(34)
150(l)	25.74(21)	−7.027(67)	−0.79(59)	−16.983(87)	−6.999(59)
160(g)	1.04(7)	−0.438(30)	1.14(7)	−17.818(56)	0.663(37)
160(l)	24.79(18)	−6.722(54)	0.87(21)	−17.878(118)	−6.690(51)
170(g)	1.58(13)	−0.630(63)	1.70(10)	−18.644(62)	0.432(94)
170(l)	23.41(25)	−6.294(66)	1.80(50)	−18.755(52)	−6.220(55)
180(g)	2.30(27)	−0.871(104)	2.40(20)	−19.497(78)	0.182(161)
180(l)	21.99(49)	−5.890(139)	2.10(30)	−19.603(158)	−5.798(153)
190(g)	3.70(53)	−1.312(170)	3.50(30)	−20.334(56)	0.358(228)
190(l)	20.72(49)	−5.539(131)	3.50(50)	−20.432(67)	−5.373(129)
200(g)	5.04(41)	−1.687(122)	4.50(20)	−21.272(21)	−0.796(158)
200(l)	18.22(124)	−4.897(299)	4.70(40)	−21.388(64)	−4.650(301)

boxes with the usual periodic boundary conditions. About 5000 simulation cycles were carried out to achieve equilibration, and additional 5000 cycles to obtain the ensemble averages, with a simulation cycle consisting of 500 particle displacements, a volume change, and 50–1000 particle transfer trial moves. The cutoff distance was set to half the box length for two-body interactions, and to a quarter of the box length for three-body interactions. Standard relations[16] were used to compensate the effects of the finite cut-off on energy, pressure, and chemical potential.

IV. RESULTS AND DISCUSSION

Simulations of the vapor–liquid phase equilibria of krypton were performed from slightly above the triple point up to the critical region. Two *ab initio* potentials, aug-cc-pV∞Z and $4d2f$-$\{2d1f\}$ were used in these simulations. For the aug-cc-pV∞Z potential, two series of simulations were performed, one with this two-body potential only and one including the AT potential, while for the $4d2f$-$\{2d1f\}$ potential simulations were performed with two-body potential only. The results of the simulations are presented in Tables IV–VI for the aug-cc-pV∞Z, aug-cc-pV∞Z plus AT, and $4d2f$-$\{2d1f\}$ potentials, respectively. Figures 3 and 4

show the results of the simulations for the densities of the coexisting phases and for the vapor pressure, respectively, together with experimental data.[17]

The critical point cannot be calculated directly by the Gibbs ensemble Monte Carlo method. However, the critical temperature can be obtained indirectly by fitting the calculated (ρ, T) coexistence data to the appropriate critical scaling law,[18]

$$\rho_1 - \rho_g = b(T_c - T)^\beta, \tag{5}$$

where $\beta \approx 0.32$ is the nonclassical critical exponent, and b and the critical temperature T_c are the adjustable parameters of the fit. Subsequently, the critical density ρ_c can be determined by fitting the equilibrium data to the law of the rectilinear diameter,[18]

$$\frac{\rho_1 + \rho_g}{2} = \rho_c + A(T - T_c), \tag{6}$$

where A and the critical density ρ_c are the adjustable parameters of the fit. The critical properties are given in Table VII and compared with experimental data.

The simulation results obtained with the aug-cc-pV∞Z potential show that the two-body potential is not able to pre-

TABLE VI. Vapor–liquid equilibria of krypton. Simulation results obtained with the $4d2f$-$\{2d1f\}$ pair potential without three-body corrections: densities, molar internal energies, vapor pressure, chemical potential, and molar enthalpies of the coexisting phases.

T/K	ρ/mol dm^{-3}	U_m/kJ mol^{-1}	p/MPa	μ/kJ mol^{-1}	H_m/kJ mol^{-1}
140(g)	0.39(4)	−0.173(19)	0.42(4)	−16.268(88)	0.904(31)
140(l)	26.93(12)	−7.495(38)	−0.09(56)	−15.860(235)	−7.502(30)
150(g)	0.60(2)	−0.249(10)	0.67(3)	−17.098(51)	0.868(14)
150(l)	26.04(17)	−7.187(62)	−0.40(37)	−16.850(151)	−7.174(71)
160(g)	1.00(13)	−0.393(48)	1.12(12)	−17.831(111)	0.736(67)
160(l)	24.84(31)	−6.798(94)	0.82(66)	−17.848(126)	−6.768(91)
170(g)	1.56(8)	−0.588(35)	1.73(7)	−18.604(39)	0.526(56)
170(l)	23.42(21)	−6.329(71)	1.37(24)	−18.710(73)	−6.274(73)
180(g)	2.33(11)	−0.842(44)	2.50(10)	−19.434(35)	0.239(48)
180(l)	22.12(36)	−5.946(108)	2.60(50)	−19.481(76)	−5.831(108)
190(g)	3.16(12)	−1.089(39)	3.30(10)	−20.340(23)	0.033(54)
190(l)	20.01(33)	−5.356(79)	3.10(9)	−20.380(58)	−5.207(64)
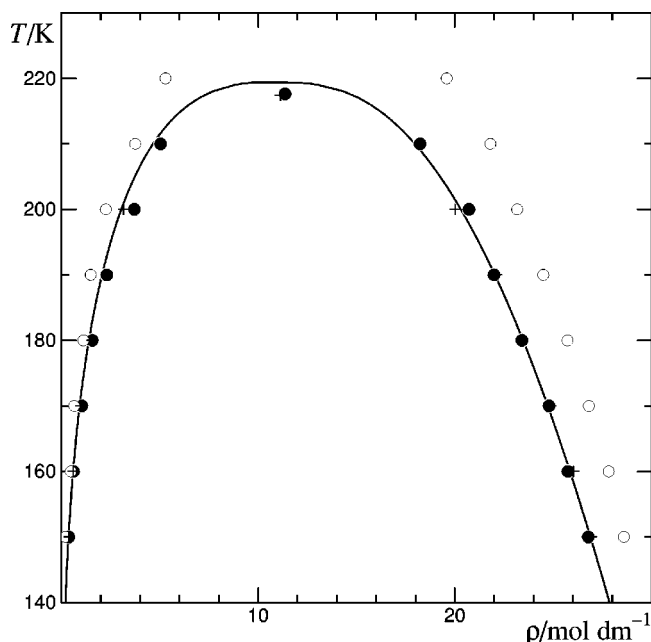
FIG. 3. Orthobaric densities of krypton. ○, computer simulation results for the aug-cc-pV∞Z potential without three-body corrections; ●, for the same pair potential plus three-body corrections; +, for the $4d2 f$-$\{2d1f\}$ potential; —, experimental data (Ref. 17).

dict the vapor–liquid phase equilibria of krypton accurately, whereas the addition of the AT potential to the configurational energy improves the results and leads to a rather good agreement with experimental data. Similar observations had been made previously with simulation studies of argon using an accurate empirical potential with and without the AT term,[19] and with global simulations of argon and nitrogen.[3,4]

The predicted critical temperature from the simulation results of the aug-cc-pV∞Z plus AT potential is only 0.89%
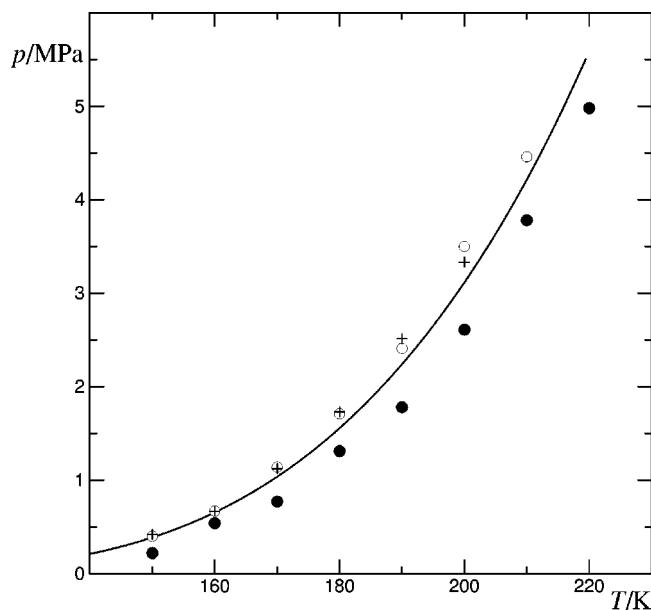
FIG. 4. The vapor pressure curve of krypton. ○, computer simulation results for the aug-cc-pV∞Z potential without three-body corrections; ●, for the same pair potential plus three-body corrections; +, for the $4d2 f$-$\{2d1f\}$ potential; —, experimental data (Ref. 17).

TABLE VII. Critical properties of krypton.

Parameter	aug-cc-pV∞Z	$4d2 f$-$\{2d1f\}$	Expt.[a]
T_c/K	207.62	207.42	209.48
ρ_c/mol dm^{-3}	11.37	11.13	10.84

[a]Reference 17.

less than the experimental value; the predicted critical density is too high by 4.89%. The simulations with the MP4 potential yield almost the same critical temperature, but a slightly better critical density (2.65% too high). At a first glance, the deviations of the predicted critical densities might seem relatively large, but one should keep in mind that they are extrapolated values. Furthermore, the experimental values differ by about 1.2% even between critically evaluated data compilations;[11,17] some primary experimental data differ even by more than 10%.[20]

The results of this section show that the aug-cc-pV∞Z potential is of high accuracy, and certainly a good basis for *ab initio* predictions of thermodynamic properties of krypton. On the other hand, the reasonably good predictions of densities of the coexisting phases, vapor pressures, and critical parameters of krypton obtained with the $4d2 f$-$\{2d1f\}$ potential show that it is an excellent effective two-body potential for krypton: The neglect of the three-body interactions in the fluid phase properties of krypton is evidently to some extent compensated by the errors caused by the MP4 perturbation theory and its $4d2 f$-$\{2d1f\}$ basis set. Of course, such a cancellation of errors can be expected for a limited range of densities and temperatures only. Indeed, the second virial coefficients predicted with the $4d2 f$-$\{2d1f\}$ pair potential are systematically too high, whereas the predictions with the aug-cc-pV∞Z potential almost coincide with the experimental data (see Fig. 2).

We conclude that the *ab initio* prediction of thermodynamic properties of fluids from quantum mechanical and statistical thermodynamic principle is possible even for a heavy atom like krypton. The coupled-cluster method, applied to correlation consistent basis sets, yields reliable pair potentials, and three-body effects can (and should) be taken into account by means of the Axilrod–Teller triple-dipole potential. The deviations of the predicted values from the experimental data are already approaching the experimental uncertainties, and it can be expected that global simulations will in some cases become an alternative to experiments.

[1] A. Z. Panagiotopoulos, J. Phys.: Condens. Matter **12**, R25 (2000).
[2] R. Eggenberger, S. Gerber, H. Huber, and M. Welcker, Mol. Phys. **82**, 689 (1994).
[3] K. Leonhard and U. K. Deiters, Mol. Phys. **98**, 1603 (2000).
[4] K. Leonhard and U. K. Deiters, Mol. Phys. **100**, 2571 (2002).
[5] F. Tao, J. Chem. Phys. **111**, 2407 (1999).
[6] S. F. Boys and F. Bernardi, Mol. Phys. **19**, 553 (1970).
[7] W. Klopper, Mol. Phys. **99**, 481 (2001).
[8] R. A. Aziz and M. J. Slaman, Mol. Phys. **58**, 679 (1986).
[9] T. Korona, L. Williams, R. Bukowski, B. Jeziorski, and K. Szalewicz, J. Chem. Phys. **106**, 5109 (1997).
[10] K. T. Tang and J. P. Toennies, J. Chem. Phys. **80**, 3726 (1984).
[11] *Thermodynamic Tables: Nonhydrocarbons*, edited by K. R. Hall (Thermodynamic Research Center, Texas A&M University, 1972).
[12] R. Bukowski and K. Szalewicz, J. Chem. Phys. **114**, 9518 (2001).
[13] B. M. Axilrod and E. Teller, J. Chem. Phys. **11**, 299 (1943).

[14] P. J. Leonard and J. A. Barker, Theor. Chem. (N.Y.) **1**, 117 (1975).
[15] A. Z. Panagiotopoulos, Mol. Phys. **61**, 813 (1987).
[16] M. P. Allen and D. Tildesley, *Computer Simulation of Liquids* (Clarendon, Oxford, 1987).
[17] N. B. Vargaftik, *Tables on the Thermophysical Properties of Liquids and Gases in Normal and Dissociated States* (Wiley, New York, 1975).
[18] B. Smit and D. Frenkel, *Understanding Molecular Simulation* (Academic, New York, 1996).
[19] J. A. Anta, E. Lomba, and M. Lombardero, Phys. Rev. E **55**, 2707 (1997).
[20] K. H. Simmrock, R. Janowsky, and A. Ohnsorge, *Critical Data of Pure Substances*, Vol. II in *DECHEMA Chemistry Data Series* (DECHEMA, Frankfurt am Main, 1986).